

## Hydrogen-Atom Abstraction Reaction of $\text{CF}_3\text{CH}_2\text{OCF}_3$ by Hydroxyl Radical

Hari Ji Singh,\* Bhupesh Kumar Mishra, and Pradeep Kumar Rao

Department of Chemistry, DDU Gorakhpur University, Gorakhpur - 273009, India. \*E-mail: hari\_singh81@hotmail.com

Received August 26, 2010, Accepted October 19, 2010

Theoretical investigations are carried out on the title reaction by means of ab-initio and DFT methods. The optimized geometries, frequencies and minimum energy path are obtained at UB3LYP/6-311G(d,p) level. Single point energy calculations are performed at MP2 and MP4 levels of theory. Energetics are further refined by calculating the energy of the species with a modified Gaussian-2 method, G2M(CC,MP2). The rate constant of the reaction is calculated using Canonical Transition State Theory (CTST) utilizing the ab-initio data obtained during the present study and is found to be  $5.47 \times 10^{-12} \text{ cm}^3 \text{ molecule}^{-1} \text{ s}^{-1}$  at 298 K and 1 atm.

**Key Words:** Theoretical chemistry, Hydrofluoroethers, Potential energy surface, Canonical transition state theory

### Introduction

It is now a well recognized fact that atomic chlorine transported to the stratosphere on account of release of a variety of chlorine containing compounds particularly chlorofluorocarbons (CFCs) into the atmosphere are responsible for the catalytic destruction of ozone in the atmosphere.<sup>1-4</sup> Chlorine atoms generated by the decomposition of CFCs in the stratospheric region through a series of catalytic reactions lead to a net decrease in the total ozone concentration in the upper atmosphere, with a net increase in ultraviolet radiation resulting in adverse effects on plants and animals. The Montreal Protocol and its continuous updates on substances that deplete the ozone layer led to a global consensus to restrict the use of chlorinated compounds on account of its deleterious effect on the environment and agreed to phase out of their production. Serious attempts have been made to find out alternatives of CFCs, and hydrochlorofluorocarbons (HCFCs) and hydrofluorocarbons (HFCs) come out as viable alternatives to chlorofluorocarbons (CFCs).<sup>5-6</sup> Studies performed with many of the HFCs and HCFCs have shown that these are not a reliable solution to protect the ozone layer. Recently hydrofluoroethers (HFEs) have been the focus of intense attention as replacement materials for CFCs and HFCs.<sup>7</sup> Hydrofluoroethers (HFEs) are being used as third generation replacements to CFCs, HCFCs and HFCs.<sup>8-9</sup> The absence of chlorine atoms in HFEs shows that such compounds would have little impact on stratospheric ozone and that they would possess a negligible ozone depleting potential (ODP).<sup>10-11</sup> However, the presence of C-F and C-O bonds in HFEs may enhance the absorption features in the atmospheric infrared region (800 - 1400  $\text{cm}^{-1}$ ) and could play a significant role as green house gases.<sup>12</sup> Therefore, considerable attention has been paid in recent years to perform experimental and theoretical studies on the decomposition kinetics of HFEs.<sup>13-16</sup>

Tropospheric degradation is expected to be initiated mainly by the attack of OH radicals in the gas phase<sup>17</sup> and  $\text{CF}_3\text{CH}_2\text{OCF}_3$  (HFE-246cb2) may undergo H atom abstraction as follows.



The reactant,  $\text{CF}_3\text{CH}_2\text{OCF}_3$  would possess  $C_s$  symmetry. Thus the two hydrogen atoms of the  $-\text{CH}_2$  position are equivalent and therefore, only one channel is identified for the title reaction as given by reaction (1).

Literature survey reveals that no experimental study is performed for this reaction yet. Thus, there is desirable need to perform theoretical studies utilizing DFT methods. In the present study we have theoretically investigated the kinetics of hydrogen atom abstraction reaction of  $\text{CF}_3\text{CH}_2\text{OCF}_3$  with OH radical. The aim of the present paper is to have a more accurate thermochemical data using modified composite method, G2M (CC, MP2). Canonical Transition State Theory (CTST) is also utilized to predict the rate constant of the title reaction on the basis of ab-initio data obtained during the present investigation.

### Computational Methods

All calculations performed during the course of the present investigation were done using the GAUSSIAN 03 suits of programs.<sup>18</sup> Amongst a series of available options B3LYP/6-311G (d,p) method was found to be sufficiently accurate for predicting reliable geometries of the stationary points. At the same time it is not computationally expensive to scan the potential energy surfaces. Therefore, geometries of reactants, products and transition state for reaction (1) were optimized at the UB3LYP/6-311G(d,p) level.<sup>19-20</sup> Vibrational frequency calculations employed for the characterization of stationary points on the potential energy surface of the title reaction have been identified to correspond to local minima with all positive values of vibrational frequencies (NIMAG = 0). Zero point energy (ZPE) corrections, and rate constant calculation were made too. Transition state is characterized by the occurrence of only one imaginary frequency (NIMAG = 1) on the potential energy surface. To confirm that there is smooth transition from reactants to products through the observed transition state structure, intrinsic reaction coordinate (IRC) calculations<sup>21</sup> were performed with the same level of theory at which optimization and frequency calculation had been performed.

In order to obtain a more refine energy values for various

species involved in reaction (1), a variant of the Gaussian-2 (G2) type methodology<sup>22</sup> has been used during the present study. Mebel *et al*<sup>23</sup> have recommended G2M(CC, MP2) version of G2 method to yield considerably accurate value for the system that contains six to seven heavy atoms.

According to the proposed scheme the geometry optimization and frequency calculation are performed at UB3LYP/6-311G(d,p) level and single point energy calculation is performed at MP2 and MP4 levels. CCSD(T)/6-311G(d,p) calculation is substituted for the QCISD(T)/6-311G(d,p) calculation of the original G2 method. The modified G2 composite method, G2M (CC, MP2) yields a composite energy as described below:

$$E[\text{G2M(CC, MP2)}] = E_{\text{base}} + \Delta E(3\text{df}, 2\text{p}) + \Delta E(\text{CC}) + \text{HLC} + \text{ZPE}$$

where,

$$E_{\text{base}} = E[\text{MP4/6-311G(d,p)}],$$

$$\Delta E(3\text{df}, 2\text{p}) = E[\text{MP2/6-311} + \text{G}(3\text{df}, 2\text{p})] - E[\text{MP2/6-311G(d,p)}],$$

$$\Delta E(\text{CC}) = E[\text{CCSD(T)/6-311G(d,p)}] - E[\text{MP4/6-311G(d,p)}],$$

$$\text{HLC (High Level Correction)} = -0.00525n_{\alpha} - 0.00019n_{\beta} \quad (n_{\alpha} \text{ and } n_{\beta} \text{ are the number of } \alpha \text{ and } \beta \text{ valence electrons with } n_{\alpha} \geq n_{\beta}), \text{ and}$$

ZPE = Zero-point energy, obtained from vibrational frequency calculation performed at UB3LYP/6-311G(d,p) level.

## Results And Discussion

The optimized geometries of reactants, products and transition state obtained at UB3LYP/6-311G(d,p) level are shown in Fig. 1. The structural parameters for  $\text{CF}_3\text{CH}_2\text{OCF}_3$ ,  $\text{CF}_3\text{CHOFC}_3$  and the transition state involved in reaction (1) are recorded in Table 1. The data show that calculated bond distances for OH and  $\text{H}_2\text{O}$  are in very good agreement with the corresponding experimental values.<sup>24-25</sup> TS structure from data recorded in Table 1 followed by visualization of the optimized geometries using GaussView<sup>26</sup> reveals that the breaking bond C-H increases from 1.091 to 1.211 Å (almost an 11% increase) whereas the newly formed H-O bond is increased from 0.972 to 1.325 Å resulting in an increase of about 38%. The fact that the elongation of forming bond is larger than that of the breaking bond indicates that the barrier of the reaction is near the corresponding reactants. This means the reaction will proceed *via* early transition state structure which is in consonance with Hammond's postulate<sup>27</sup> applied to an exothermic hydrogen abstraction reaction. These results are in accord with that obtained in an earlier study performed at MP2 level by Sun *et al*<sup>28</sup> for H atom abstraction reaction in a similar Hydrofluoroethers,  $\text{CF}_3\text{CHFOCH}_3$  in which they found an increase of C-H bond distance from 1.097 to 1.196 Å (9%) in the transition state structure together with an elongation in the H-O bond distance from 0.958 to 1.320 Å (37.8%). In another computational study conducted by Yang *et al*<sup>29</sup> on another similar compound  $\text{CHF}_2\text{CH}_2\text{OCF}_3$ , the analysis of transition state for H atom abstraction reaction revealed

the stretching of the breaking C-H bond by 10.5% at B3LYP/6-311G(d,p) while H-O bond distance increased by 35.7%.

Results obtained during frequency calculations for species involved in reaction (1) and the corresponding transition state are recorded in Table 2. These results show that the reactants and products have stable minima on their potential energy surface characterized by the occurrence of only real positive vibrational frequencies. Transition state (TS) is characterized by the occurrence of only one imaginary frequency (**886i**) as recorded in Table 2. Visualization of the vibration corresponding to the calculated imaginary frequencies using GaussView program<sup>26</sup> shows a well defined transition state geometry connecting reactants and products during transition. The existence of transition state on the potential energy surface is further ascertained by intrinsic reaction coordinate (IRC) calculation performed at the same level of theory using the Gonzalez-Schlegel steepest descent path<sup>21</sup> in the most weighted Cartesian coordinates with a step size of 0.01 (amu<sup>1/2</sup> · bohr). Force constants at 41 selected points (21 points in the reactant channel and 20 points in the product channel) and the geometries were optimized along the minimum energy path. The IRC plot for TS is shown in Fig. 2 that clearly shows a smooth transition from reactants to products on the potential energy surface.

Single point energy calculations of various species involved in the abstraction reaction (1) were performed using MP2, MP4 and CCSD(T) level of theories at UB3LYP/6-311G(d,p) optimized geometries. Calculated total energies are corrected for zero-point energy obtained at UB3LYP/6-311G(d,p) and corrected with a scale factor of 0.96.<sup>30</sup> Zero-point corrected total

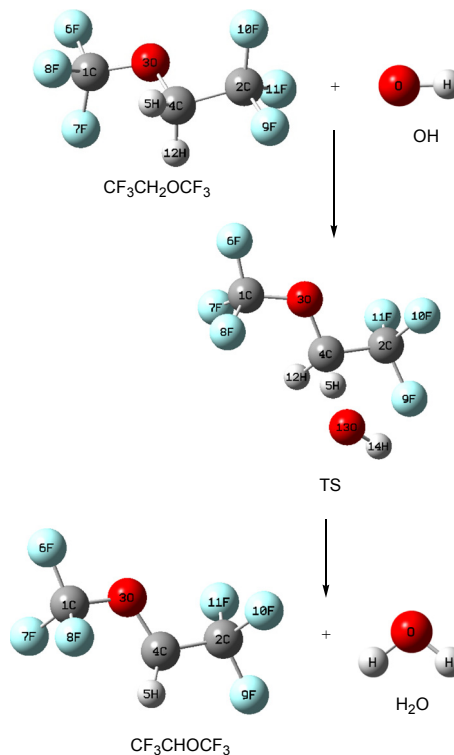


**Figure 1.** Optimized geometries of reactants, products and transition state involved in the H-atom abstraction reaction of  $\text{CF}_3\text{CH}_2\text{OCF}_3$  by OH radical using UB3LYP/6-311G(d,p) method.

**Table 1.** Structural parameters of  $\text{CF}_3\text{CH}_2\text{OCF}_3$ ,  $\text{CF}_3\text{CHOFC}_3$  and TS involved in reaction (1) at the UB3LYP/6-311G(d,p) level of theory

	$\text{CF}_3\text{CH}_2\text{OCF}_3$	TS	$\text{CF}_3\text{CHOFC}_3$	OH	$\text{H}_2\text{O}$
Bond length (Å)					
R (O-H)				0.967 <sup>a</sup>	0.962 <sup>a</sup>
				0.970 <sup>b</sup>	0.958 <sup>b</sup>
R (C1-F6)	1.326	1.324	1.322	-	-
R (C1-F7)	1.350	1.346	1.338	-	-
R (C1-F8)	1.350	1.340	1.342	-	-
R (C2-F9)	1.349	1.354	1.346	-	-
R (C2-F10)	1.341	1.336	1.355	-	-
R (C2-F11)	1.341	1.343	1.344	-	-
R (C2-C4)	1.516	1.514	1.483	-	-
R (C1-O3)	1.347	1.361	1.368	-	-
R (C4-O3)	1.428	1.402	1.366	-	-
R (C4-H5)	1.091	1.211	1.080	-	-
R (C4-H12)	1.091	1.090	-	-	-
R (O13-H14)	-	0.972	-	-	-
R (O13-H5)	-	1.325	-	-	-
Bond Angle (deg)					
A (O-H-O)	-	-	-	-	103.8 <sup>a</sup>
					104.4 <sup>b</sup>
A (C2-C4-O3)	107.244	108.694	114.036	-	-
A (C2-C4-H5)	108.633	106.773	121.014	-	-
A (C2-C4-H12)	108.633	110.848	-	-	-
A (F6-C1-F7)	108.727	108.953	109.375	-	-
A (F6-C1-F8)	108.727	109.337	109.231	-	-
A (F9-C2-F10)	108.048	108.139	107.445	-	-
A (F9-C2-F11)	108.048	108.140	108.017	-	-
A (O3-C1-F6)	108.244	107.652	107.498	-	-
A (O3-C1-F7)	112.239	111.644	111.589	-	-
A (C4-C2-H9)	108.428	106.453	109.014	-	-
A (C4-C2-H10)	112.050	112.291	112.721	-	-
A (C4-C2-H11)	112.050	111.916	112.110	-	-

<sup>a</sup>Values obtained during present study. <sup>b</sup>Experimental values taken from Ref. 24 and 25.

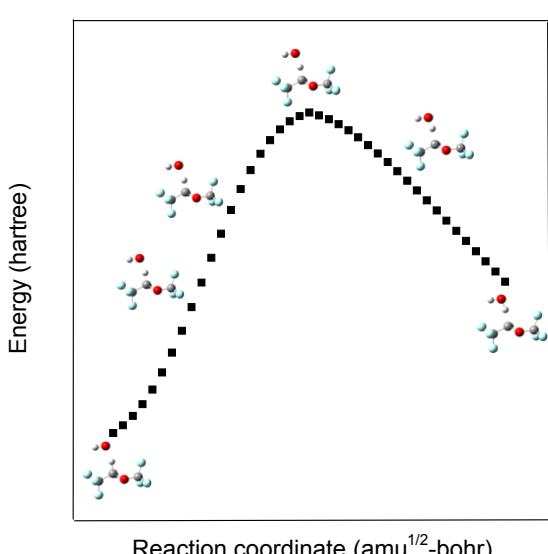
**Table 2.** Vibrational frequencies of reactants, products and transition state at UB3LYP/6-311G(d,p) level of theory

Species	Vibrational frequencies ( $\text{cm}^{-1}$ )
$\text{CF}_3\text{CH}_2\text{OCF}_3$	10, 54, 123, 135, 213, 325, 354, 430, 452, 531, 538, 609, 616, 630, 701, 853, 891, 974, 1102, 1155, 1173, 1193, 1220, 1280, 1312, 1316, 1451, 1503, 3068, 3127
TS	886, 25, 47, 58, 87, 123, 175, 178, 216, 329, 346, 431, 444, 530, 539, 586, 611, 616, 694, 699, 789, 876, 904, 972, 1149, 1159, 1178, 1196, 1213, 1288, 1300, 1314, 1393, 1502, 3113, 3738
$\text{CF}_3\text{CHOFC}_3$	21, 46, 105, 122, 213, 323, 336, 427, 452, 479, 538, 591, 610, 623, 635, 710, 877, 899, 1111, 1176, 1186, 1194, 1206, 1279, 1304, 1455, 3226
OH	3707 (3735) <sup>a</sup>
$\text{H}_2\text{O}$	1638, 3810, 3907 (1595, 3657, 3756) <sup>b</sup>

The experimental values are shown in parenthesis. <sup>a</sup> - Ref. 34. <sup>b</sup> - Ref. 35.

**Table 3.** Zero-point corrected total energy at different level of theory for the reactants, products and transition state along with the associated energy barrier,  $\Delta E$  in kcal/mol. All other values are in hartree

Level	$\text{CF}_3\text{CH}_2\text{OCF}_3 + \text{OH}$	TS	$\text{CF}_3\text{CHOFC}_3 + \text{H}_2\text{O}$	$\Delta E$
MP2/6-311G(d,p)	-863.826731	-863.814085	-863.851556	7.93
MP2/6-311+G(3df, 2p)	-864.344590	-864.333043	-864.377056	7.24
MP4/6-311G(d,p)	-863.922937	-863.911605	-863.942783	7.10
CCSD(T)/6-311G(d,p)	-863.911899	-863.903123	-863.931927	5.50
G2M(CC, MP2)	-864.676978	-864.669414	-864.704697	4.74

**Figure 2.** IRC plot for the transition state (TS) involved in  $\text{CF}_3\text{CH}_2\text{OCF}_3 + \text{OH}$  reaction at UB3LYP/6-311G(d,p) method.

energies using standard and extended basis sets for various species and transition state involved in the title reaction calculated with different computational methods are recorded in Table 3. The associated energy barrier corresponding to reaction (1) calculated from the results obtained at various level of theories are also recorded in Table 3. These results show that energy barriers for H atom abstraction reaction of  $\text{CF}_3\text{CH}_2\text{OCF}_3$  with hydroxyl radical are in the range of 4.7 to 7.9 kcal mol<sup>-1</sup> depending upon the level of theories involved during the calculation. The barrier height for title reaction calculated in this work tends to decrease with an increase in the size of the basis set and also with the treatment of electron correlation. Literature survey reveals that there is no experimental data available for the comparison of the energy barrier for the H-atom abstraction reaction of  $\text{CF}_3\text{CH}_2\text{OCF}_3$  by OH radical. However, to ascertain the reliability of the calculated value a comparison is made with the value calculated by Yang *et al.*<sup>29</sup> for a structurally similar compound  $\text{CHF}_2\text{CH}_2\text{OCF}_3$  using MC-QCISD//B3LYP/6-311G(d,p) method yielding a value of 4.10 kcal mol<sup>-1</sup>. Using approximately a same level of theory in the present study, the G2M(CC, MP2), an energy barrier of 4.74 kcal mol<sup>-1</sup> is obtain-

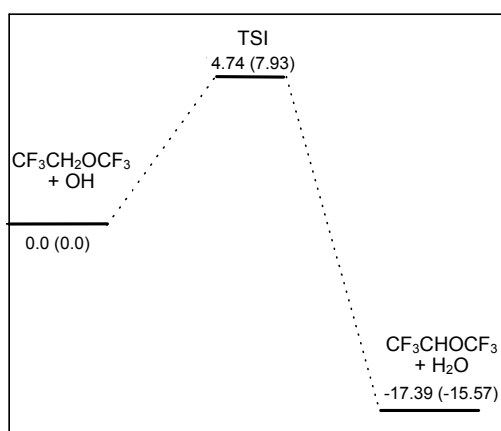


**Figure 3.** Potential energy diagram of the title reaction. The values in parentheses are ZPE corrected total energies at MP2/6-311G(d,p) level. Energy values are in kcal/mol.

ed for the  $\text{CF}_3\text{CH}_2\text{OCF}_3\text{H}$  atom abstraction by OH radical. On the other hand, G3(MP2) calculation of Sun *et al*<sup>28</sup> resulted in a value of 5.03 kcal mol<sup>-1</sup> for H atom abstraction reaction in another similar compound,  $\text{CF}_3\text{CHFOCH}_3$ . These values are in a very good agreement with our calculated value. This gives us a confidence that the single point energy calculation data obtained using G2M(CC, MP2) method on the geometries optimized at UB3LYP/6-311G(d,p) level would yield precisely accurate energy barrier for H-atom abstraction reaction of  $\text{CF}_3\text{CH}_2\text{OCF}_3$  by hydroxyl radical. A potential energy diagram of the title reaction is constructed with the results obtained at the G2M(CC, MP2)//B3LYP/6-311G(d,p) level and is shown in Fig. 3. In the construction of energy diagram zero-point corrected total energy data as recorded in Table 3 are utilized. These energies are plotted with respect to the ground state energy of  $\text{CF}_3\text{CH}_2\text{OCF}_3$  arbitrarily taken as zero. The values in parentheses shown in Fig. 3 are ZPE corrected values obtained at MP2/6-311G(d,p) level. The results show that the calculation performed during the present study utilizing composite G2 method, G2M(CC, MP2) yields the lowest barrier height of 4.74 kcal mol<sup>-1</sup>. Spin contamination is not important for the  $\text{CF}_3\text{CH}_2\text{OCF}_3$  because  $\langle S^2 \rangle$  is found to be 0.76 at UB3LYP/6-311G(d,p) before annihilation that is only slightly larger than the expected value of  $\langle S^2 \rangle = 0.75$  for doublets.

### Rate Constants

The rate constant for reaction (1) is calculated using Canonical Transition State Theory (CTST)<sup>31</sup> that involves a semi-classical one-dimensional multiplicative tunneling correction factor given by the following expression:

$$k = \Gamma(T) \frac{k_B T}{h} \frac{Q_{\text{TS}}^{\ddagger}}{Q_R} \exp \frac{-\Delta E}{RT} \quad (2)$$

where  $\Gamma(T)$  is the tunneling correction factor at temperature T.  $Q_{\text{TS}}^{\ddagger}$  and  $Q_R$  are the total partition functions for the transition state and reactants respectively.  $\Delta E$ ,  $k_B$  and  $h$  have their usual

meaning. We adopted the simple and computationally inexpensive Wigner's method<sup>32</sup> for the estimation of the tunneling correction factor using the expression

$$\Gamma(T) = 1 + \frac{1}{24} \left( \frac{h\nu^{\#}}{k_B T} \right)^2 \quad (3)$$

where  $\nu^{\#}$  is the imaginary frequency at the saddle point. The tunneling correction factor  $\Gamma(T)$  is found to be almost unity. The partition functions for the respective transition state and reactants at 298 K are obtained from the vibrational frequencies calculation made at UB3LYP/6-311G(d,p) level. The rate constant for H atom abstraction reaction of  $\text{CF}_3\text{CH}_2\text{OCF}_3$  by OH as given by reaction (1) is calculated to be  $5.47 \times 10^{-12} \text{ cm}^3 \text{ molecule}^{-1} \text{ s}^{-1}$  at 298 K and 1 atm. Literature survey reveals that there is no experimental data available to make a comparison with the value obtained during the present investigation. However, the calculated rate constant is compared with the data available for similar hydroxylfluoroethers studied theoretically and experimentally by independent group of workers. Oyaro *et al*<sup>33</sup> studied the OH +  $\text{CF}_3\text{CH}_2\text{OCH}_3$  in a smog chamber utilizing RR-GC/MS method and determined the rate constant to be  $5.9 \times 10^{-13} \text{ cm}^3 \text{ molecule}^{-1} \text{ s}^{-1}$  at 298 K. On the other hand a theoretical investigation by Yang *et al*<sup>29</sup> for a similar hydroxylfluoroether,  $\text{CHF}_2\text{CH}_2\text{OCF}_3$ , the corresponding rate constant was estimated to be  $2.74 \times 10^{-14} \text{ cm}^3 \text{ molecule}^{-1} \text{ s}^{-1}$  at 298 K. Our calculated value is about 1 to 2 order of magnitude larger than these values. As a result we expect that the present study may provide useful information for future laboratory investigations.

### Conclusions

The potential energy surface and reaction kinetics of the H atom abstraction reaction of  $\text{CF}_3\text{CH}_2\text{OCF}_3$  with OH radical are investigated at G2M(CC,MP2)//UB3LYP/6-311G(d,p) level of theory. The barrier height for this pathway is calculated to be 4.74 kcal mol<sup>-1</sup>. The thermal rate constant for the H atom abstraction of  $\text{CF}_3\text{CH}_2\text{OCF}_3$  by OH radical is found to be  $5.47 \times 10^{-12} \text{ cm}^3 \text{ molecule}^{-1} \text{ s}^{-1}$  at 298 K and 1 atm using Canonical transition state theory.

**Acknowledgments.** The authors are thankful to University Grants Commission, New Delhi for providing fellowships to BKM and PKR under its DSA/BSR program sanctioned to the Department of Chemistry, DDU Gorakhpur University, Gorakhpur.

### References

1. Solomon, S. *Nature* **1990**, *347*, 6291.
2. Molina, M. J.; Rowland, F. S. *Nature* **1974**, *249*, 810.
3. Rowland, F. S.; Molina, M. J. *Chem. Eng. News* **1994**, *8*, 72.
4. Weubbles, D. J. *J. Geophys. Res.* **1983**, *88*, 1433.
5. Scientific Assessment of Stratospheric Ozone, Vol 11, World Meteorological Organization Global Ozone Research and Monitoring Project report No-20 (WMO, Geneva), 1989.
6. Wayne, R. P. *Chemistry of Atmospheres*; Clarendon press: Oxford,

- 2001.
7. Tsai, W. T. *J. Hazard Mater.* **2005**, *119*, 69.
  8. Sekiya, A.; Misaki, S. *J. Fluorine Chem.* **2000**, *101*, 215.
  9. Bivens, D. B.; Minor, B. H. *Int. J. Refrig.* **1998**, *21*, 567.
  10. Ravishankara, R. A.; Turnipseed, A. A.; Jensen, N. R.; Barone, S.; Mills, M.; Howark, C. J.; Solomon, S. *Science* **1994**, *263*, 71.
  11. Granier, C.; Shine, K. P.; Daniel, J. S.; Hansen, J. E.; Lal, S.; Stordal, F. *Climate Effects of Ozone and Halocarbon Changes*; In Scientific Assessment of Ozone Depletion, 1998; Rep. 44, Global Ozone Research and Monitoring Project, World Meteorological Organization, Geneva, Switzerland, 1999.
  12. Good, D. A.; Francisco, J. S. *J. Phys. Chem.* **1998**, *102*, 1854.
  13. Chen, L.; Kutsuna, S.; Tokuhashi, K.; Sekiya, A. *J. Phys. Chem. A* **2006**, *110*, 12845.
  14. Urata, S.; Takada, A.; Uchimaru, T.; Chandra, A. K. *Chem. Phys. Lett.* **2003**, *368*, 215.
  15. Chen, L.; Kutsuna, S.; Tokuhashi, K.; Sekiya, A.; Takeuchi, K.; Ibusuki, T. *Int. J. Chem. Kinet.* **2003**, *35*, 239.
  16. Good, D. A.; Kamboires, M.; Santiano, R.; Francisco, J. S. *J. Phys. Chem. A* **1999**, *103*, 9230.
  17. Wallington, T. J.; Schneider, W. F.; Sehested, J.; Blide, M.; Platz, J.; Nielsen, O. J.; Christensen, L. K. *J. Phys. Chem. A* **1997**, *101*, 8264.
  18. Frisch, M. J. et al. Gaussian 03 (Revision C.02); Gaussian Inc.; Wallingford, CT, 2004.
  19. Becke, A. D. *J. Chem. Phys.* **1993**, *98*, 5648.
  20. Lee, C.; Yang, W.; Parr, R. G. *Phys. Rev.* **1988**, *37*, 785.
  21. Gonzalez, C.; Schlegel, H. B. *J. Chem. Phys.* **1989**, *90*, 2154.
  22. Curtiss, L. A.; Raghavachari, K.; Trucks, G. W.; Pople, J. A. *J. Chem. Phys.* **1991**, *94*, 7221.
  23. Mebel, A. M.; Morokuma, K.; Lin, M. C. *J. Chem. Phys.* **1995**, *103*, 7414.
  24. In NIST Chemistry Web Book, NIST Standard Reference Database Number 69, Release (Constants of Diatomic Molecules data compiled by K.P. Huber and G. Herzberg), website: <http://www.ccbdb.nist.gov/>, 2005.
  25. Kuchitsu, K. *Structure of Free Polyatomic Molecules Basic Data*; Springer-Verlag: Berlin, Vol 1, p 58, 1998.
  26. Frisch, A.; Nielsen, A. B.; Holder, A. J. *GaussView Users Manual*, Gaussian Inc, 2003.
  27. Hammond, G. S. *J. Am. Chem. Soc.* **1955**, *77*, 334.
  28. Sun, H.; Gong, H.; Pan, X.; Hao, L.; Sun, C. C.; Wang, R.; Huang, X. *J. Phys. Chem. A* **2009**, *113*, 5951.
  29. Yang, L.; Liu, J.; Li, Z. *J. Chem. Theory Comput.* **2008**, *4*, 1073.
  30. Scott, A. P.; Radom, L. *J. Phys. Chem.* **1996**, *100*, 16502.
  31. Truhlar, D. G.; Garrett, B. C.; Klippenstein, S. J. *J. Phys. Chem.* **1996**, *100*, 12771.
  32. Wigner, E. P. *Z. Phys. Chem.* **1932**, *B19*, 203.
  33. Oyaro, N.; Sellevag, S. R.; Nielsen, C. J. *J. Phys. Chem. A* **2005**, *109*, 337.
  34. Shimanouchi, T. In *Tables of Molecular Vibrational Frequencies Consolidated*; Vol 1, National Bureau of Standards: U.S. GPO, Washington, 1972.
  35. In NIST Chemistry Web Book, NIST Standard Reference Database Number 69, (Vibrational frequency data compiled by T. Shimanouchi), website: <http://www.ccbdb.nist.gov/>, 2005.